ELSEVIER

Journal of Chromatography B, 694 (1997) 333–341

JOURNAL OF CHROMATOGRAPHY B

In vivo determination of 5-bromo-2′-deoxyuridine incorporation into DNA tumor tissue by a new ^{32}P-postlabelling thin-layer chromatographic method

Jacob J. Steinberg*, Gary W. Oliver Jr. , Nazih Farah, Payman Simoni, Raz Winiarsky, Antonio Cajigas

Unified Division of the Autopsy, Departments of Pathology and Radiation Oncology, Albert Einstein College of Medicine, Montefiore Medical Center, C-312, 111 East 210th Street, Bronx, New York, NY 10467, USA

Received 30 May 1995; revised 29 November 1996; accepted 9 December 1996

Abstract

The halopyrimidine 5-bromo-2′-deoxyuridine (BUDR) can serve as one of many indicators of tumor malignity, complementary to histologic grade. We have developed a thin-layer chromatographic (TLC) technique that can assess tumor DNA base composition and analogue (BUDR) incorporation which vies with immunochemistry for BUDR. This requires post-labeling DNA by nick-translation and radioactive 5′-phosphorylation of representative ^{32}P-α-dNMPs (deoxynucleotide monophosphates). Subsequent 3′-monophosphate digest exchanges a radioactive $^{32}PO_4$ for the neighboring cold nucleotide. Separation in two dimensional PEI-cellulose TLC is carried out in acetic acid, $(NH_4)_2SO_4$, and $(NH_4)HSO_4$. TLC of dNMPs was applied to control HeLa DNA, and HeLa cells receiving BUDR. BUDR is detected in 10^6 HeLa cells after 12–72 h incubations. Findings in HeLa DNA demonstrate normal TLC retention factors for all ^{32}P-dNMPs. Two dimensional R_F (*x,y* axes in cm) demonstrate: dAMP=1.4, 9.4; dCMP=10.0, 13.5; dGMP=4.6, 4.4; dTMP=9.0, 7.4; and BUDRMP 6.4, 6.6. This technique quantifies BUDR-which parallels tumor S phase, and serves as an indicator of labelling index (LI). © 1997 Elsevier Science B.V.

Keywords: HeLa cells; 5-Bromo-2′-deoxyuridine; DNA

1. Introduction

Studies on DNA ploidy and cytometry have attempted to improve DNA S-phase activity commonly employed in determining cancer virulence. The halopyrimidine nucleoside, 5-bromo-2′-deoxyuridine (BUDR) offers one of many opportunities for determining tumor growth [1–3]. In brief, BUDR: (1) can be used in patients in-hospital or on an outpatient setting [4,5]; (2) does not require expensive equipment, e.g., computerized flow cytometry; (3) does not need complicated tumor tissue preparation; (4) pre-operative dosages of BUDR are relatively low risk [6]; (5) complementary immunohistochemistry is easily done on prepared slides, and combined results correlate with flow cytometry [7], and BUDR-ELISA; (6) BUDR labelling index (LI)

*Corresponding author.

PII S0378-4347(97)00051-0

is acceptably synonymous with S phase and correlates with aneuploidy [8–10]; (7) BUDR DNA uptake is an indicator of labelling index in tumor/host microenvironment as opposed to in vitro clonogenic assays; (8) BUDR correlates with histologic grading [4,5,11,12]; (9) BUDR is a radiosensitizer if additive radiation therapy is contemplated [13]; (10) BUDR labelling can couple with other chemotherapies prior to tumor excision, and can generate a chemotherapeutic-kill BUDR labelling index [14]; (11) BUDR correlates with receptor negative status in breast cancers (high LI; [3]); (12) can affect surgical therapy: if BUDR LI is low, it questions the need for additional lymph node dissection [6]; (13) can affect decisions regarding adjuvant therapy host [15]; (14) lastly, BUDR labelling may correlate with clinical course [16–19].

We have developed a reproducible two-dimensional thin layer chromatographic (2D-TLC) technique that identifies and separates BUDRMP from other deoxynucleotides (dNMPs; [20]). The applications of this technique to detect BUDR are many, but an easily appreciated example is its utility in cancer chemotherapy [21,22]. Empirical techniques are now employed to decide how much chemotherapy a patient receives, e.g., calculated by body weight and surface area. Yet, patients vary in their abilities to tolerate chemotherapies. This could result in under- or over-dosing patients. Further, chemotherapies are expensive, and more individual dosing could be cost saving. This assay helps fashion a more custom-designed regimen, based on analogue uptake. The quantification of BUDR in DNA may be carried out by assaying lymphocytic DNA, sperm DNA, or by a small tissue or cytopathologic needle biopsy (the assay of a few thousand cells).

The present 2D-TLC technique which enhances the ability to detect BUDRMP (BUDR-monophosphate) is based on a technique which has been presented in detail. The technique labels representative fractions of all dNMPs in DNA, in situ, affording adduct and analogue detection. The TLC separation retains normal dNMPs retention values, which allows rapid visual assessment by characteristics R_F values, and of BUDRMPs content in DNA [22]. This may allow better drug monitoring which can effect tumor resistance, and/or host toxicity.

2. Experimental

Nucleic acids: calf thymus DNA (Type I; highly polymerized), 2′-deoxy-5′-nucleotides (dAMP, dCMP, dGMP, dTMP, dATP, dCTP, dGTP, dTTP), and BUDR-5′-triphosphate as cold phosphate controls, were purchased from Sigma Chemicals (St. Louis, MO, USA). Alpha- ^{32}P-radiolabeled (3000 uCi/mmol; 8–16 uCi per nick) dATP, dCTP, dGTP, and dTTP were purchased from Amersham, or New England Nuclear (Dupont, Cambridge, MA, USA). Transfer ribonucleic acid (tRNA) from Type XXI/*Escherichia coli*, strain W, was purchased from Sigma.

Enzymes: Micrococcal nuclease (EC 3.1.31.1; activity: 100–200 μmolar units per mg of protein), and spleen phosphodiesterase II (EC 3.1.16.1; activity: 13.5 units per mg of protein) were purchased from Sigma. DNase I, and *Escherichia coli* DNA-polymerase I were purchased from Boehringer–Mannheim (Indiannoplis, IN, USA).

Chromatographic solvents and plates: first dimension: 1 *M* acetic acid, pH adjusted to 3.5 with NaOH was purchased from J.T. Baker, (Phillipsburgh, NJ, USA). Second dimension: 74 g of $(NH_4)_2SO_4$, 0.4 g of $(NH_4)HSO_4$ (Aldrich, Milwaukee, WI, USA) and 4 g of Na_2EDTA in 100 ml of dH_2O. TLC plates, polyester polyethyleneimine cellulose were purchased from Machery–Nagel–Merck, (Sigma).

Reagents: precipitants and buffers (commonly available): 100% ethanol, 70% ethanol, TE buffer at pH 8.0, PBS buffer; DNA digest buffer: 20 m*M* succinate, and 8 m*M* calcium chloride at pH of 6.0.

Equipment: laser densitometry is by Beckmann Instruments (New York, NY, USA); Phosphoro-imager from Mitsubishi (White Plains NY, USA) and TLC scintillation counter via a computerized Ambis (Boston, MA, USA). Kodak XAR-5 film (20.3×25.4 cm) by Eastman Kodak Company (Rochester, NY, USA). Computerized nuclear and cellular measurement was carried out by the CAS 200 (San Diego, CA, USA)

Cell culture media: purchased from Sigma.

Kits: DNA extraction ASAP columns and nick translation kits were purchased from Boehringer–Mannheim.

3. Methods

Substrate DNA, ^{32}P-labeling and nick-translation methods for TLC analysis of formed-DNA adducts and analogues: this technique of detection is sensitive from one adduct per 10^5 to 10^8 deoxynucleotides, and has been explained in detail [20,21].

Partial replacement of dTMP by BUDRMP: 2 μl of unlabeled BUDR as the cold triphosphate (1.8×10^{-9} moles/μl) was added to standard nick-translation of control calf thymus DNA.

Cell culture: HeLa cell culture by standard methods.

Cellular measurements: were accomplished by a CAS-200 by standard computer programs. These measurements included: DNA mass (pg), DNA index (ploidy vs. control), area (μm^2), nucleolar area, mass, shape (complexity of geometry: low number under 10=round; higher numbers 11–50: crenated, folded, sausage and hockey shapes, etc.), and DNA density (from control). A minimum of 100 cells per treatment were measured.

DNA: freshly extracted human HeLa DNA.

Ambis or Phosphoro-imager computer assisted TLC scintillation counting: this is carried out directly after drying the second phase. Typical readings require 15–30 min, and chromatograms are reproduced. Controls are added to the TLC plate to establish quenching, which is significant below 500 DPM (1:10). A linear regression to control for quenching generated the equation of $Y=0.51X-945$ ($r^2=0.999$), where Y is CPM from Ambis, and X is true DPM based on standard ^{32}P controls.

Beckmann laser densitometry computer assisted analysis of the TLC XAR-5 autoradiograms: this has been as sensitive as scintillation counting and is helpful in determining analogue to deoxynucleotide ratios, retention factor, quantification of proximate adducts to known dNMPs, area of spot exposure, and spot density (on gray scale) which reflects quantity of each labeled phosphate. The ability to graphically superimpose each film with control spots ultimately simplifies the analyses of product. All R_F values are presented as the consequent two-dimensional R_x values {X,Y coordinates}, and converted to exact R_F values by the formula $(R_x-1)/19$.

4. Results

The results of the following TLCs are presented and discussed to include: (1) schematic of 2D-TLC with relative mobilities (R_F values) for control DNA and DNA containing BUDRMP which partially replaces dTMP (Fig. 1): the schematic demonstrates mobility in the first and second dimension of a DNA digest to dNMPs. DNA samples may contain deoxyuridylate (dUMP; open oval). Deoxy-5′6′-dihydroxythymidylate (thymidylate glycol; TG) migrates rapidly in the second dimension and maybe present in DNA exposed to oxidative stress. Other examples of abnormal dNMPs, i.e., adducts, that are formed through oxygen stress include 8-hydroxyguanidylate (8-OH-dGMP), which migrates below dGMP, and 5-hydroxymethyluridulate (HmdUMP), which migrates above and eccentric to dAMP-and may partially overlap methylated dAMPs.

The halopyrimidine analogue, BUDR, once incorporated into DNA, is easily detected below at a 7 o'clock position to dTMP. This is a unique R_F and is easily detected at very low DPM (less than 50), or after appropriate autoradiography.

Other phosphates within the field may represent normal minor base nucleotides present in DNA, e.g., normally methylated dNMPs, or adducts, and by-products of oxygen stress. Typical autoradiography not only demonstrates four primary spots, but is accompanied by a specific pattern for each dNMP analogues replaced in DNA from chemotherapeutically treated cell line.

(2) Control human HeLa DNA: findings for control HeLa DNA digest include (Fig. 2): 1. Normal retention factors of all radio-labeled monophosphates to cold UV-markers. Autoradiogram demonstrates, in clockwise position, the migration pattern of a HeLa DNA digest as their deoxyribonucleotides (Table 1; retention factor is given as a bi-coordinate location {R_x} X,Y in cm): dAMP=1.4, 9.4; dCMP=10.0, 13.5; dGMP=4.6, 4.4; dTMP=9.0, 7.4. Our percentages of dNMP label of calf thymus DNA are tabulated (Table 1). Deoxyuridylate (dark arrow) exists after 24 h autoradiography which may represent an artefactually chemically altered product of dCMP, or is likely real. (A potential neighbor to dTMP is deoxyinosine 3′-

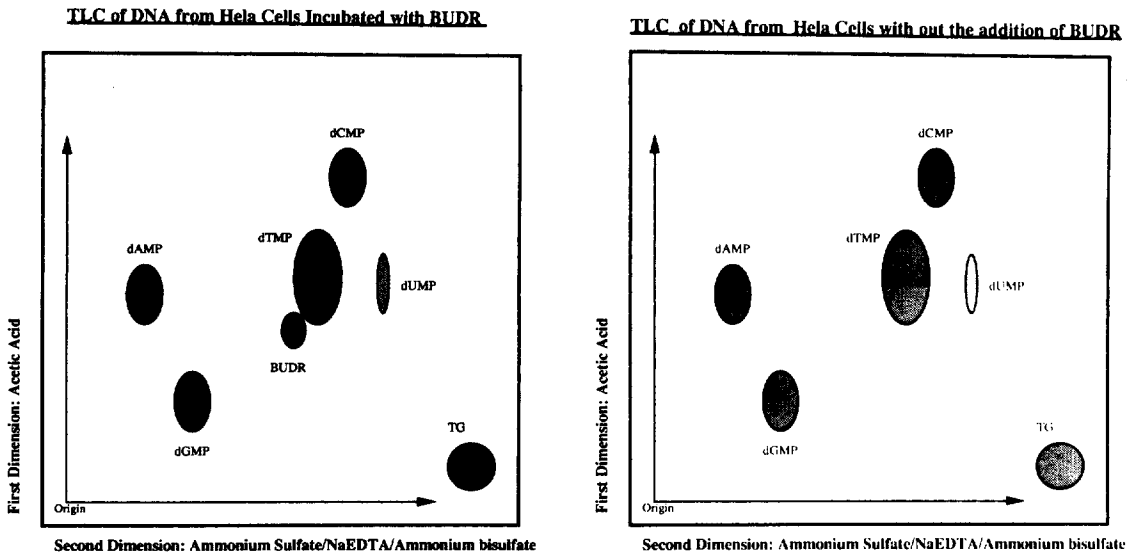

Fig. 1. Schematic of 2D-TLC with relative R_F values for control DNA and DNA containing BUDRMP which partially replaces dTMP. The schematic demonstrates mobility in the first and second dimensions of a DNA digest to dNMPs. DNA samples may contain deoxyuridylate (dUMP; open oval). TG migrates rapidly in the second dimension. The halopyrimidine analogue, BUDR, once incorporated into DNA, is easily detected below at a 7 o'clock position to dTMP.

Fig. 2. Control human placental DNA: Autoradiogram demonstrates, in clockwise position, the major bases of DNA as their nucleotides. Two dimensional R_F values (X,Y axes in cm) demonstrate: dAMP =1.4, 9.4; dCMP=10.0, 13.5; dGMP=4.6, 4.4; dTMP=9.0, 7.4.

monophosphate, which is eliminated by the addition of deoxycorfomycin – the gift of Dr. Vern Schramm, Department of Biochemistry, Albert Einstein College of Medicine, NY, USA). After 72 h autoradiography, four additional minor spots, if present, may be more visible in many human DNA samples: 5-me-dAMP, two spots close to dCMP representing 5-me-dCMP, and dUMP. Human placental DNA is essentially devoid of methylated bases and dUMP – not surprising in rapidly dividing DNA repair proficient placental cells. Over-labeling of dTMP is consistent in nick-translation, and can be used to better define nearest neighbor base composition (Table 1). Further, some variation in DPM exists due to differences in quenching at lower counts (10:1 at 200 DPM) vs. higher counts (2:1 over 10 000 DPM). Lastly, densitometry integrates area, and not gray scale density on the autoradiogram, and these numbers appear in Table 1.

(3) Cold stoichiometric replacement of BUDRMP for dTMP: (Fig. 3; 24 h autoradiogram): we have been able to detect BUDRMP on our TLCs. BUDR is enzymatically incorporated into DNA, and migrates below dTMP (densitometry R_x–BUDRMP 6.4, 6.6; densitometry percentage 47.1% at highest,

Table 1
Densitometry vs. scintillation counting: tabular results of dNMP percentages from in vitro control HeLa DNAs

Nucleotides	Hela control	Hela Br-dUTP
R_x values		
dAMP	1.4/9.4	2.5/10.6
dCMP	10.0/13.5	11.9/14.1
dGMP	4.6/4.4	3.9/5.0
dTMP	9.0/7.4	7.8/10.5
Br-dUMP	–	6.4/6.6
Area (mm^2)		
dAMP	485	484
dCMP	421	225
dGMP	371	361
dTMP	968	346
Br-dUMP	–	871
Percent volume ($AUmm^2$)		
dAMP	31.44%	15.34%
dCMP	8.49%	10.07%
dGMP	14.04%	12.99%
dTMP	46.02%	4.64%
Br-dUMP	–	56.97%
AMBIS		
dAMP	25701/29.2%	7208/16.9%
dCMP	11254/12.8%	4632/10.9%
dGMP	9303/10.6%	5379/12.6%
dTMP	41621/47.4%	5352/12.5%
Br-dUMP	–	20097/47.1%

Linear regression coefficients predict interchangeable results from densitometry to Ambis.

in vitro, m*M* substitution). Ambis detects significant counts of BUDRMP. BUDRMP has a unique autoradiographic chromatographic pattern. Few other confounding autoradiographic densities are evident. The five pointed star at 2 o'clock to dAMP likely represents HmdUMP. Spots along the *Y* axis likely represent inorganic monophosphate moieties (typically with low R_x values) or nucleic acid monophosphates (higher R_x values) with molecular masses in excess of 600–800. Fig. 2 demonstrates our ability to detect these abnormal cold dNMPs from normal. The addition of BUDR after incorporation into DNA, significantly competes with dTMP labeling.

(4) Cold stoichiometric replacement of BUDRMP for dTMP: a 3-D representation (Fig. 4; 15 min Ambis, computer constructed): BUDRMP uptake appears as a dominant peak obliterating the view of dTMP – which it has effectively competed against. The light shadow above dAMP at 2 o'clock likely

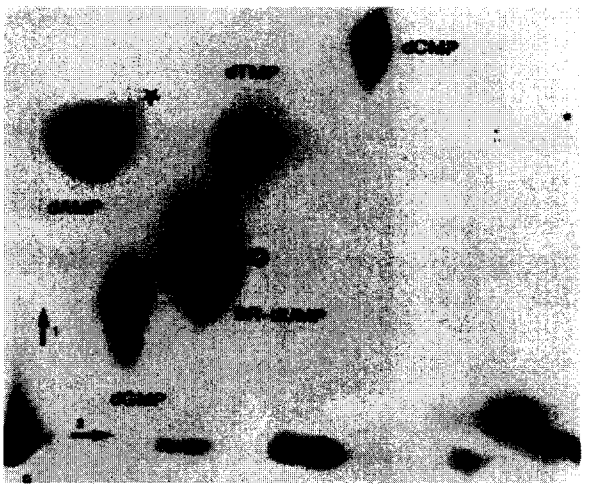

Fig. 3. Cold stoichiometric replacement of BUDRMP for dTMP: BUDR is easily enzymatically incorporated into DNA, and migrates below dTMP (densitometry R_x–BUDRMP=6.4, 6.6). The five pointed star at 2 o'clock to dAMP likely represents HmdUMP. Spots along the *Y* axis likely represent inorganic monophosphate moieties (typically low R_x values) or nucleic acid monophosphates (higher R_x values) with molecular masses in excess of 600–800.

represents HmdUMP. Rapid Ambis assessment of the TLC plate is sensitive to significant peaks, and many autoradiographic spots evident along the *X* (Fig. 2) axis are not evident.

(5) HeLa and cold BUDR labeling–Phosphoro-imager detection (Fig. 5): phosphoro-imaging may enhance rapid, sensitive detection of analogues, adducts and normal dNMPs. The ability of computer coupled phosphoro-imaging to digitally enhance areas of interest on the chromatogram is demonstrated by a high power view of the area that encompasses dGMP, dAMP and dTMP – which surrounds BUDRMP.

(6) Histogram labeling index (LI; ×100) of cell culture treated with incremental BUDR over time (Fig. 6): the ability of cells to incorporate BUDR is dose and time dependent. Cell resistance to BUDR is based on the cytosine deaminase content of tumor cells–which can be overcome by the use of tetrahydouridine (THU; non-competitive inhibitor) or the addition of cytosine/cytidine (dC; competitive inhibitor). Both THU and dC will increase BUDR incorporation into DNA.

Results demonstrate, at low levels of BUDR (16

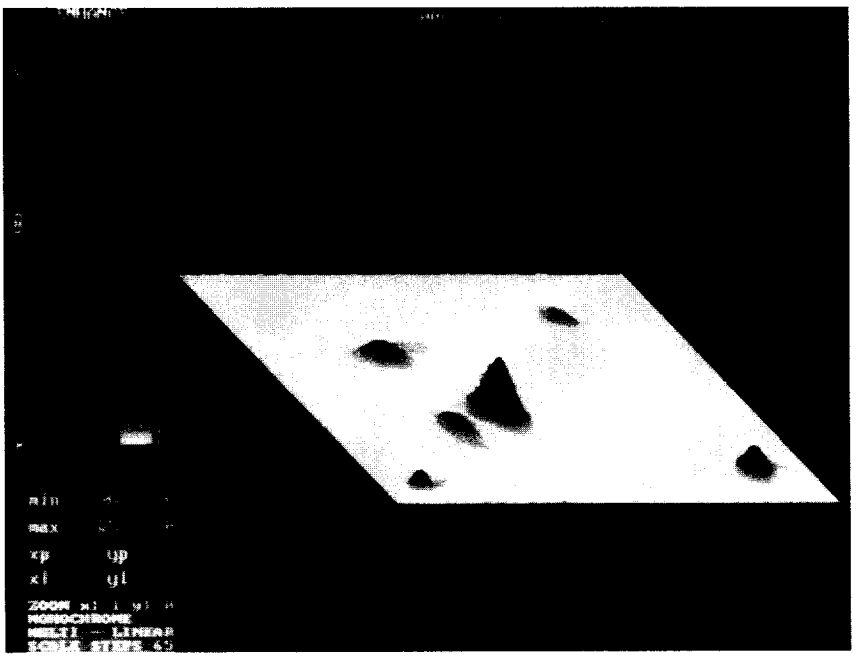

Fig. 4. Cold stoichiometric replacement of BUDRMP for dTMP: a 3-D representation (Fig. 3; 15 min Ambis, computer constructed): BUDRMP uptake appears as a dominant peak obliterating the view of dTMP which it has effectively competed against. The light shadow above dAMP at 2 o'clock likely represents HmdUMP.

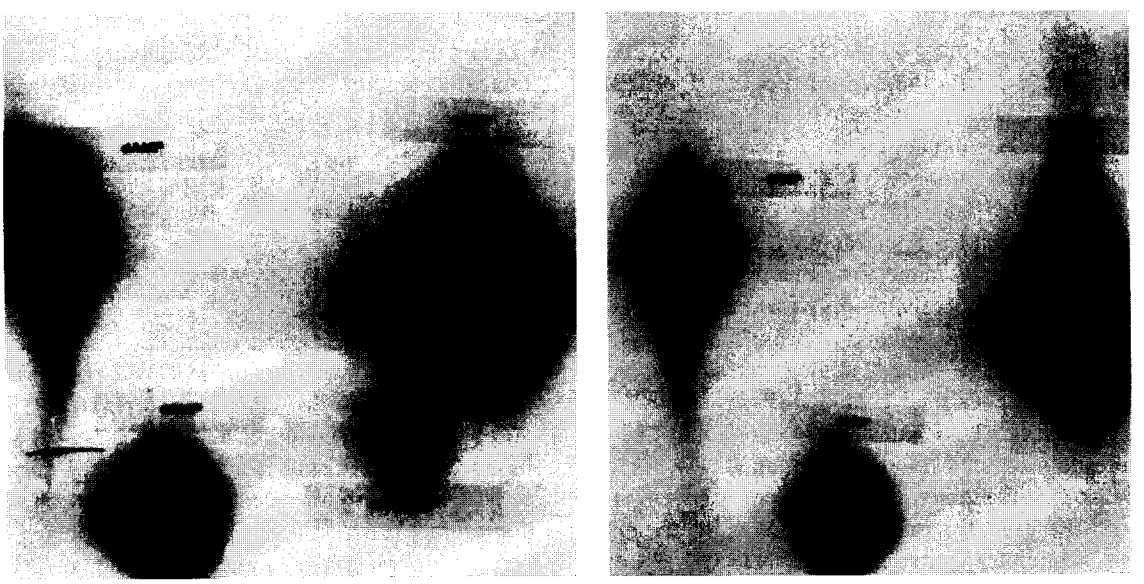

Fig. 5. HeLa and cold BUDR labeling–Phosphoro-imager detection. The ability of computer coupled phosphoro-imaging to digitally enhance areas of interest on the chromatogram is demonstrated by a high power view of the area that encompasses dGMP, dAMP and dTMP–which surrounds BUDRMP. This data can be available within 15 min.

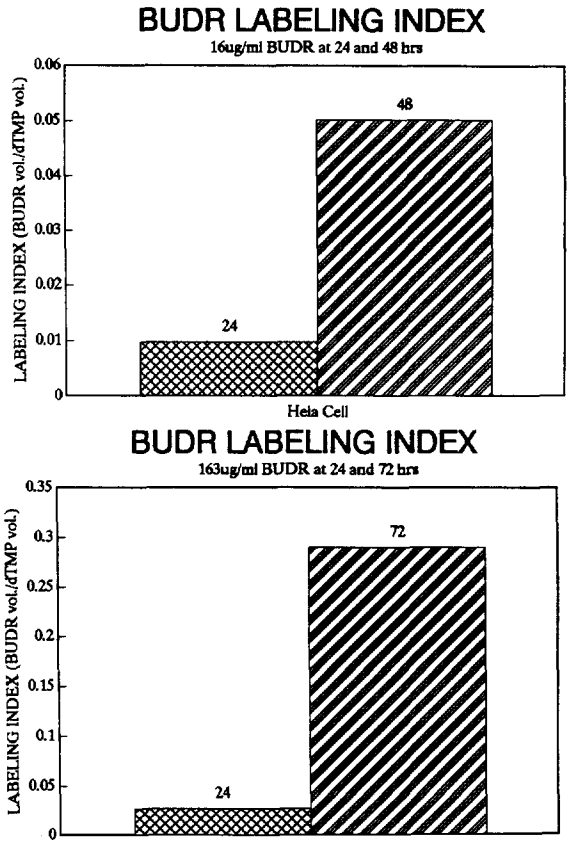

Fig. 6. Histogram labeling index (LI; ×100) of cell culture treated with incremental BUDR over time: results demonstrate at low levels of BUDR (16 μg; 24–48 h) an LI of 1% and 5%, respectively. LI increases significantly over time and at higher concentrations of BUDR (163 μg; 24–72 h) to 3% and 29%, respectively.

μg; 24–48 h), an LI of 1% and 5%, respectively. LI increases significantly over time and at higher concentrations of BUDR (163 μg; 24–72 h) to 3% and 29%, respectively.

Table 1, in vitro results: densitometry vs. scintillation counting. Ambis correlated closely with densitometry, but exceeded densitometry percent by 11% overall when viewed by dNMP across DNA samples (inter-DNA variability). Variability in analysis of DNAs (all dNMPs in one DNA vs. another DNA) was much less and densitometry here exceeded Ambis by only 4%. Correlation coefficients still tend to be extremely small, yet very significant

Fig. 7. Photomicrograph (Giemsa stain for nuclear detail; 40×) of BUDR treated HeLa cells displays features of both treated and untreated cells. Larger, massively cytomegalic cells with prominent and multiple nucleoli are related to drug effect and BUDR incorporation into DNA. Many other large cells display nucleoli with aberrant geometric shapes. Smaller cells are more characteristic of transformed, untreated cervical HeLa cells.

($P<0.001$). Linear regression coefficients predict interchangeable results from densitometry to Ambis.

Cellular measurements by CAS-200 measurement (Fig. 7), BUDR treated HeLa cells had a higher DNA index from untreated cells (4.2 untreated vs. 8.4 BUDR-treated, with a control of 2); had double the DNA content (30 pg vs. 60.6 pg); and almost double the volume (111.4 vs. 218.8 u^2). BUDR treated cells had nucleoli that ranged in size from 30–89 u^2 vs. control of up to 30 u^2. Nucleolar shape tended to be more aberrant with attributed number of up to 42-designating for geometric complexity and variation in shape more than normal. Some of this represents chemotherapeutic effects and selection of cell type.

5. Discussion

Wacker discovered 5-bromouracil (BrU) can be incorporated into DNA in *Streptococcus faecalis*. BrU caused hot spots and mutations in phage T4 [23]. BrU is a thymine base analogue and acts as a radiosensitizer. Within DNA, BrU reacts like cytosine and pairs with guanine [24]. Bromouracil is better tolerated in DNA than other halopyrimidines

due to bromines van der Waals radius (r=0.195), which is close to the methyl (r=0.200) of thymine. Iodine atom (r=0.215 nm) and chlorine (r=0.180 nm) are less well tolerated. Fluorine (r=0.135 nm) approaches hydrogen (0.120 nm; 25]. DNA is inactivated by gamma radiation or ultraviolet light more easily if it contains BrU-a sensitization that occurs with all halopyrimidines. This can also diminish DNA repair [27]. Cells vary in their sensitivity to BUDR, and mouse leukemia cells L5178Y are quite sensitive to halopyrimidines in their DNA [25]. No sensitizing effect occurs if the halopyrimidine is not incorporated into DNA [26], though free bromine may attack the 2-deoxyribose sugar at the C-1 forming a 2-deoxy-d-ribonolactone-which is then detected by its alkali lability [25].

Deoxynucleotide analogues are enzymatically introduced into DNA by the use of anti-metabolite chemotherapies, e.g., halopyrimidines and deoxydeazapurines [21]. Aside from BUDR, the present 2D-TLC technique can successfully quantify many DNA analogues and adduct formation. The procedure requires labeling extracted cold DNA (so no radioactivity is injected into the patient) by random radioactive 5′-phosphorylation of representative ^{32}P-alpha-dNMPs from a patient who has received BUDR. Subsequent 3′-monophosphate digests the DNA and exchanges a radioactive $^{32}PO_4$=to the neighboring cold dNMP-now radioactively labelling the cold DNA dNMPs and BUDR from the patient. Separation is easily and reproducibly carried out with two dimensional thin layer chromatography. The experience with this technique exceeds 2000 chromatograms with statistically significant reproducibility, e.g., R_F variation under 5%.

5.1. Clinical application

Historical data on labelling indices are based on tritiated thymidine. The clinical applicability of this as a tool for calculating doubling time remains mostly in cell culture. Cell culture is an artificial environment for a tumor, and cannot completely reflect the host-tumor microenvironment. The option of giving large amounts of tritiated thymidine to a patient is both expensive, and may pose risk in disposing of human radioactive waste. The administration of cold BUDR bypasses these obstacles. It is taken into DNA readily, the labelling index of BUDR is interchangeable with tritiated thymidine, and minimal hazard is posed to the patient.

BUDR can help determine DNA index (DI; [28]]. This is the ratio of DNA in G1 population versus normal diploid cells. The DI may reflect the degree of malignancy and possibly local aggressiveness. Some association to survival, e.g., diploid vs. aneupolid, is likely. Labelling Index (LI) is another measure calculated from BUDR uptake – which measures the proportion of cells synthesizing DNA. To date this required in vitro incubation of cells with tritiated thymidine, and autoradiography. Cell death effects and long tritium autoradiography delays this process. Definitions of LI and tumor grade fall into the categories of low, <0.25%, medium=0.26–4.0%, and high 4–12%. Adjuvant chemotherapy may benefit a patient with a high LI. LI is valuable and independent of TNM stage, receptors, ploidy, or host status, e.g., menopausal. Human protocols for BUDR typically require sampling 7 h after infusion of 200 mg BUDR (other human protocol include: 500 mg in 100 ml 0.9% saline IV over 30 min and 6 h before biopsy; animal studies require 100 mg/kg IP, 8.5 prior to biopsy) [28]. Delayed sampling may yield no results since metabolic dehalogenation takes place. Occasionally arterial infusion is employed, and plasma levels range from 1–7 μM. LI in brain tumors arterially infused range from 2–26%. IUDR, a close analogue of BUDR, levels are achieved by infusing 1000 mg/m^2/day for 14 days prior to irradiation [29]. Radioactive IUDR-remains in the blood for 10 h, and is constant in tissue for a day or more, then declines. One can increase BUDR uptake by tetrahydrouridine which inhibits cytidine deaminase [29]. In animals with L1210 cells, the half life of BUDR is 5 days after an IP injection. For in vitro tumor studies, BUDR is added at 15.4 μg/ml (50 μM) for sister chromatid exchange (SCE)–an indicator of genetic fragility. Fresh tumor samples may only need 15 μM. BUDR renders cells and hosts light sensitive – so cells should be kept in the dark [30].

The benefits of this thin layer chromatographic technique have been outlined previously. In brief, they are: (1) the improved ability to radiolabel deoxynucleotide adducts versus standard post-labeling or antibody techniques; (2) high resolution on TLC: one employs a new TLC plate with each TLC;

(3) ease of technique with commonly available reagents and buffers; and (4) excellent quantification of low molecular weight adducts. The TLC separation between BUDRMPs and standard dNMPs contrasts the various mobilities of the halogenated pyrimidines. Weakly adsorbing moieties migrate farther. The TLC cellulose binds nitrogen better than carbon, since saturated hydrocarbons are poorly adsorbed. Adsorption is highest for –COOH> –OH> $-NH_2$> C=O> O-alkyl> –CH3 for the lowest. Also, tautomeric n7 shifts by a transient rearrangement of bonding may shift the usual configuration. These chemical re-arrangements further enhance and contrast separations that effect the ratio of carbon vs. nitrogen.

6. Summary

Our conclusions from these TLC studies are that we can quantifiably determine BUDR incorporation in genomic DNA. The technique is able to measure DNA chemotherapy analogue accumulation in tumor. It may offer an additional biomarker of tumor cell drug resistance and host sensitivity, which may effect the chemotherapeutic regimen.

Acknowledgments

Our thanks to Mr. Mark Moosikaswan for technical assistance. Supported in part by the American Federation for Aging Research, and a training and research grant from the National Cancer Institute.

References

[1] D.S. Schultz and R.J. Zarbo, Am. J. Clin. Pathol., 98 (1992) 291.
[2] J.S. Meyer, J. Nauert, S. Koehm and J. Hughes, J. Histochem. Cytochem., 37 (1989) 1449.
[3] B. Lloveras, S. Edgerton and A.D. Thor, Am. J. Clin. Pathol., 95 (1991) 41.
[4] R. Nemoto, K. Hattori, K. Uchida, T. Shimazui, Y. Nishijima, K. Koiso and M. Harada, Cancer, 66 (1990) 509.
[5] R. Nemoto, K. Uchida, T. Shimazui, K. Hattori, K. Koiso and M. Harada, J. Urol., 141 (1989) 337.
[6] T. Kamata, Y. Yonemura, K. Sugiyama, S. Ooyama, T. Kosaka, A. Yamaguchi, K. Miwa and I. Miyazaki, Cancer, 64 (1989) 1665.
[7] G.D. Wilson, N.J. McNally, S. Dische, M.I. Saunders, C. Des Rochers, A.A. Lewis and M.H. Bennett, Br. J. Cancer, 58 (1988) 423.
[8] M. Tachibana, N. Deguchi, S. Jitsukawa, S. Baba, M. Hata and H. Tazaki, J. Urol., 145 (1991) 963.
[9] A. Riccardi, M. Danova, P. Dionigi, P. Gaetani, T. Cebrelli, G. Butti, G. Mazzini and G. Wilson, Br. J. Cancer, 59 (1989) 898.
[10] A. Riccardi, M. Danova, G. Wilson, G. Ucci, P. Dormer, G. Mazzini, S. Brugnatelli, M. Girino, N.J. McNally and E. Ascari, Cancer Res., 48 (1988) 6238.
[11] F. Labrousse, C. Daumas-Duport, L. Batorski and T. Hoshino, J. Neurosurg., 75 (1991) 202.
[12] T. Hoshino, M. Prados, C.B. Wilson, K.G. Cho, K.S. Lee and R.L. Davis, J. Neurosurg., 71 (1989) 335.
[13] T.J. Hegarty et al., Int. J. Radiat. Oncol. Biol. Phys., 19 (1990) 421.
[14] M. Poot, A. Schuster and H. Hoehn, Biochem. Pharmacol., 41 (1991) 1903.
[15] I.C. Henderson, N. Engl. J. Med., 326 (1992) 1774.
[16] B. Lloveras, P. Garin-Chesa, A. Myc and M. Melamed, Am. J. Clin. Pathol., 101 (1994) 703.
[17] T. Fujimaki et al., Cancer, 67 (1991) 1629.
[18] S. Ohyama, Y. Yonemura and I. Miyazaki, Cancer, 65 (1990) 116.
[19] T. Nishizaki et al., J. Neurosurg., 73 (1990) 396.
[20] J.J. Steinberg, A. Cajigas and M. Brownlee, J. Chromatogr., 574 (1992) 41.
[21] J.J. Steinberg, G. Oliver and A. Cajigas, J. Chromatogr., 612 (1993) 277.
[22] J.J. Steinberg, G. Oliver and A. Cajigas, TLC Chromatography, Marcel Dekker, New York, Ch. 26.
[23] C. Auerbach, in A. Hollaender (Editor), Chemical Mutagens, Vol. 3, Plenum Press, New York, 1973, Ch. 24, pp. 1–19.
[24] A. Wacker, P. Chandra, G.E.W. Wohlstenholme, M. O'Connor (Editors), Mutation as Cellular Process (Ciba Foundation Symposium), Vol. 171, Churchill, London, 1964.
[25] C. von Sonntag, The Chemical Basis of Radiation Biology, Vol. 10, Taylor and Francis, London, 1987, p. 321.
[26] J.D. Regan, R.B. Setlow and A. Hollaender (Editors), Chemical Mutagens, Vol. 3, Plenum Press, New York, 1973, p. 29.
[27] M. Quintiliani, Panel Proceedings Series, Advances in Chemical Radiosensitizers, International Atomic Energy Agency, Vienna, 1974, p. 87.
[28] N.J. McNally, Int. J. Radiat. Biol., 56 (1989) 777.
[29] J.B. Mitchell, A. Russo, J.A. Cook, K.L. Straus and E. Glatstein, Int. J. Rad. Biol., 56 (1989) 827.
[30] Technical Report 260, International Atomic Energy Agency, Vienna, 1986, Ch. 7, p. 28.